A comparison of wear behaviour of heat resistant steel engine valves and TiAl engine valves

Fuqiang Lai[1,2], Shengguan Qu[1*], Haidi Qin[1], Roger Lewis[2], Tom Slatter[2], Xiaoqiang Li[1], Huahuan Luo[3]

1. Guangdong Key Laboratory for Advanced Metallic Materials Processing, School of Mechanical and Automotive Engineering, South China University of Technology, Guangzhou 510640, Guangdong, China

2. Department of Mechanical Engineering, The University of Sheffield, Mappin Street, Sheffield, UK, S1 3JD

3 Huaiji Dengyun Auto-parts (Holding) CO., LTD. Huaiji County 526400, Guangdong, China

Abstract:

The increasingly demand for higher performance internal combustion engines (ICEs) has led to higher temperatures in the combustion chamber. As a result, TiAl valves have been investigated with a view to their use in a natural gas fuelled diesel ICE, taking advantage of their low density and good high temperature resistance. In this work, comparison bench tests for traditional steel valves and TiAl valves were carried out through the use of specially designed wear testing apparatus. Compared to the traditional valves made from heat resistant steel (X60, X85), the TiAl valves have 50 % lower mass, leading to a decrease in the impact seating forces during the engine operation. With the reduction of the inertia of engine valve movement, the dynamic characteristics of the engine valve train system can be optimized. Each contact pair of valve and seat insert was tested for 3 million impact cycles. Compared to the austenitic exhaust valves (X60) tested at 700 °C, the TiAl valve had better wear resistance and the wear loss decreased by 24.8 %. The predominant wear mechanism is considered to be a combination of oxidative wear

Corresponding Author*: Shengguan Qu, Professor; E–mail: qusg@scut.edu.cn.

and adhesive wear. However, for the intake valves tested at 400 °C, the wear loss of the TiAl valve was three times higher than the martensitic intake valves (X85). The predominant wear mechanism can be identified as abrasive wear and adhesive wear. It is therefore concluded that the TiAl exhaust valve is a potential solution for a natural gas fuelled diesel.

Key words: engine valve; TiAl alloy; wear test; wear behaviour

1. Introduction

The valve and valve seat insert are critical components of the valve train, which is in turn the most important system in an internal combustion engine (ICE), as it controls the gas flow and the timing of the engine [1, 2]. One of the main design objectives for an ICE is an increase in the specific power output, however, this often leads to higher combustion chamber temperatures that cause premature failure of exhaust valves, in particular. Meanwhile, lightweight design is one of the most important development trends of the engine industry, due to the increasingly high requirements of fuel efficiency and strict emission regulations. Many new materials and designs have been developed for engine valves. However, it was difficult to obtain substantial weight reductions through the use of traditional heat resistant steel or nickel-base or cobalt-base super alloys. Thus, TiAl alloy is becoming a potential material with its low density and excellent mechanical properties at elevated temperatures, albeit with higher raw material and manufacturing costs [3]. TiAl alloys are considered as important candidate materials for advanced applications in aerospace, as well as the automotive industry [4, 5].

Engine valves are the products of mass-production with high precision. The valves made from traditional heat resistant steel are generally manufactured by hot forming and machining. However, since the low ductility and poor formability of TiAl alloy, it is not easy to produce

TiAl valves by hot forming. Research has already been carried out, however, to produce a TiAl valve with low cost and high production efficiency through different manufacturing methods [5, 6]. Other work has reported that centrifugal casting combined with a mechanical machining process was found to be a viable method [7–9]. Furthermore, the TiAl valves can be also manufactured by powder metallergy technology [10].
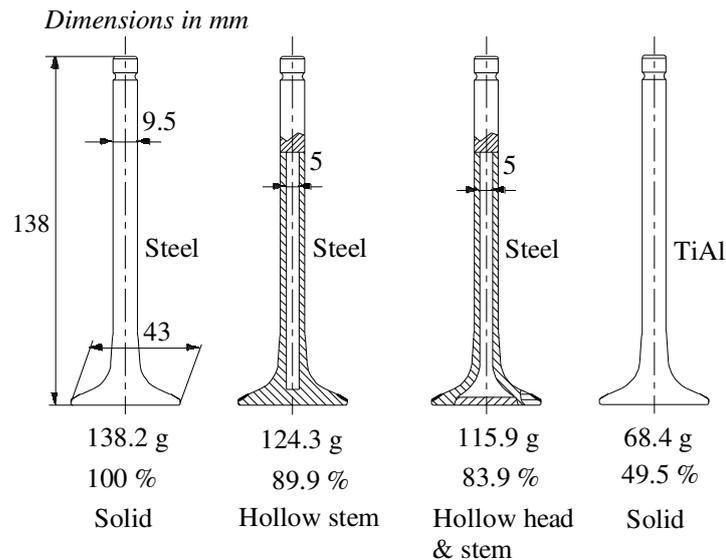
Fig. 1 Mass comparison of valves with different materials and configurations.

Fig. 1 presents the masses of valves typically used in a medium duty natural gas fuelled engine with different materials and configurations. The solid exhaust valve made of heat resistant steel is being used in a natural gas fuelled engine. The hollow stem and sodium filled valve and hollow head and sodium filled valve were manufactured and developed by Huaiji Dengyun Auto-parts (Holding) CO., LTD [11, 12]. The mass of a hollow valve is 83.9 %. of the mass of the solid valve. However, the mass of a TiAl valve would be further decreased to 49.5 %. The mass of the valves is a small proportion of the total mass of an ICE, but they occupy a large proportion of the valve train system (moving) mass. With the reduction of valve mass, the stiffness of valve spring can also be reduced, leading to a decrease in noise and impact seating

forces [5]. Consequently, the severe contact conditions between valves and seat inserts could be mitigated to some extent. A further benefit, due to the reduction of the inertia of the engine valves, is that the dynamic characteristics of the valve train system could be significantly improved (e.g. its ability to respond user demand), leading to increase in fuel economy.

Some research on TiAl engine valves has been carried out in a dynamometer engine test [5, 9, 10]. For instance, Maki et al. reported that the TiAl prototype valve demonstrated excellent high-temperature performance and wear resistance under the very severe conditions of a durability test on an actual fired engine [5]. Ouyang et al. performed 48 hour comparative tests on a diesel engine [9]. It is also reported that the valve recession of TiAl exhaust engine valves is 12.5 % of that for heat resistant steel engine valve (21-4N). However, it is reported by Li and Luo [10], that the valve recession of TiAl exhaust valves was almost the same as the original exhaust valve recession in a diesel. Unfortunately, the corresponding detailed wear behaviour and wear mechanisms have yet to be presented and discussed in published literature.

Therefore, in the work presented in this paper, wear tests for heat resistant steel engine valves and TiAl engine valves were carried out through the use of specially designed wear testing apparatus. Stress analysis of the valve specimens during the durability tests was performed using a finite element method (FEM), and the sliding distance was calculated. After the test, the wear loss from the seating face of the valve and seat insert were quantified through use of a profilometer. The worn seating faces were characterized using scanning electron microscopy (SEM), energy–dispersive spectroscopy (EDS) and wear behaviour and wear mechanisms were evaluated.

2. Experimental details

2.1 Materials

In modern engines, martensitic steels are generally used for the intake valves, and austenitic alloys and super alloys are used for exhaust valves. In this work, martensitic steels of 85Cr18Mo2V (X85) and 45Cr9Si2 steel were used for the intake valves and the valve stem of exhaust valves, respectively. Austenitic steel 61Cr21Mn10Mo1V1Nb1N (X60) was used for the valve head of the exhaust valves. In addition, valve specimens with the same geometry of the intake valve and exhaust valve were made of a TiAl alloy. The nominal chemical compositions of the engine valve materials and seat inserts are presented in Table 1. The mechanical properties of the X85 and X60 steel at high temperature were obtained using an ultimate tensile testing machine, and the mechanical properties of TiAl alloy refer the work reported by Badami et al. [3] and Maki et al. [5], as listed in Table 2. The Young's modulus of X60 at 700 °C was only 136 GPa, which was significantly lower than the Young's modulus of X85 at 400 °C (197 GPa). It should be noted that TiAl alloy could obtain quite outstanding mechanical properties at the high temperature [5]. Compared the temperature at 400 °C to the temperature at 700 °C, tensile strength of TiAl alloy kept the similar values, its Young's modulus slightly decreased from 160 GPa to 151 GPa, and the hardness reduced from 280 HV to 270 HV. However, at the temperature range lower than 700 °C, the elongation of TiAl was at low levels, indicating its low formability. The hot hardness of the engine valve and seat insert materials are listed in Table 3. It should be noted that the hardness at elevated temperatures refers to the results reported by Wang [1] and Maki et al. [5].

The details of the four valve specimens are presented in Table 4. The heat resistant steel valves

were produced by traditional hot forming and a mechanical machining process, whereas the

TiAl valves were manufactured through centrifugal casting and mechanical machining process.

Compared to the heat resistant steel valve, the mass of TiAl valve decreased to be 50 % lighter.

In order to increase the wear resistance of the valve stem and the peening and wear resistance of

the valve head seating surface, surface treatments are generally introduced [1, 5]. For instance,

the valve stem of Valve 1 was made of 45Cr9Si3 steel, and the surface of valve stem was

enhanced by chromium plate. The valve seating face of Valve 1 was nitrided. The nitriding

process was performed by salt bath liquid nitriding at 580 °C for 35 to 40 minutes. Additionally,

the seating face of Valve 3 was quenched, leading to the hardness of surface varied from 48 to

56 HRC, and the depth of hardening was 0.5 to 2.0 mm with 390 HV. After the quenching

treatment, the hardness of the seating face of Valve 3 was significantly higher than the hardness

of matrix material.

Table 1 The nominal compositions of the engine valve specimens and seat inserts (wt. %).

	C	Si	Mn	Ni	Cr	Mo	V	Cu	Fe	Ti	Others
X60	0.65	0.21	10.40	0.45	20.65	0.79	0.79	0.02	Bal.	–	N: 0.37; Nb: 1.06
45Cr9Si3	0.44	2.92	0.33	0.15	8.58	–	–	0.15	Bal.	–	–
X85	0.81	0.31	0.47	–	18.1	2.26	0.39	0.13	Bal.	–	–
TiAl	–	0.1-0.2	–	–	1.0-1.3	–	–	–	–	Bal.	Al: 30-34; Nb: 4.0-5.0; W: 4.0-5.0
Seat insert	0.9-1.1	0.3-0.5	0.4-0.5	1.2-1.4	5.0-5.3	12.0-12.5	1.0-1.2	13.0-15.0	Bal.	–	W: 3.0-3.3; Co: 4.5-5.5

Table 2 Mechanical properties of engine valve materials [3, 5].

	Temperature (°C)	σ_b (MPa)	σ_s (MPa)	Young's modulus (GPa)	Elongation (%)
X85	400	958	791	197	10.45
TiAl	400	570	–	160-165	~ 3
TiAl	700	572	~ 470	151	~ 3.5
X60	700	634	341	136	22.51

Table 3 Hot hardness of the engine valve and seat insert [1, 5].

	25 °C	400 °C	500 °C	600 °C	700 °C
X85	320 $HV_{0.2}$	–	–	–	–
TiAl	305 HV (5kgf)	280 HV (5kgf)	275 HV (5kgf)	270 HV (5kgf)	270 HV (5kgf)
X60	403 $HV_{0.2}$	~ 350 HV	~ 250 HV	~ 160 HV	–
Seat insert	462 $HV_{0.2}$	> 300 HV	–	–	–

Table 4 Details of the valve specimens.

Valve name	Valve type	Valve stem material	Valve head material	Valve seating face material	Valve weight (g)
Valve 1	Exhaust valve	45Cr9Si3, chroming	X60	X60, nitriding	153.6
Valve 2	Exhaust valve	TiAl, polishing	TiAl	TiAl, polishing	76.5
Valve 3	Intake valve	X85, chroming	X85	X85, quenching	162.8
Valve 4	Intake valve	TiAl, polishing	TiAl	TiAl, polishing	80.9

2.2 Wear apparatus and test conditions

Comparison wear tests for the four valve and seat insert contact pairs were carried out on a

bench-top wear testing apparatus, which is presented in Fig.2 (a). The power of the apparatus was supplied by a motor and was transmitted to the eccentric wheel with inner bearing by a belt. The push rod moves up and down with the rotation of the eccentric wheel. The load cell was installed between the push rod and the transfer cylinder, and the transfer cylinder transferred the heat and load to the valve head. The apparatus is more thoroughly described in the previous work [13]. The valve and seat insert geometry are illustrated in Fig.2 (b). The initial shape of the seat inserts was a result of a grinding and lapping process. Seating faces with 30° angles are often used in applications where the combustion products have little or no lubricating properties [1]. A low seat angle (24.5°) is used on the seating surface of the intake valve and seat insert for improved wear resistance. The initial contact widths of the intake and exhaust seat inserts were 2.0 mm and 2.2 mm, respectively, because, as most of the heat of a conventional solid valve is transferred to the engine cooling system through its paired seat insert with the other route mainly through the valve guide [14], the higher contact width used in the exhaust valve is helpful to promote the heat transfer. After the comparison wear tests, the worn seating surface of the valves and seat inserts were measured using a 2D contact profilometer, as indicated in Fig.2 (c). All the measurements were conducted at four points at 90° intervals.

In general, the combustion load and impact frequency have a significant influence on the wear behaviour of valves and seat inserts. In the research work of Chun et al. [15], a load of 1.96 kN was used, which was below the equivalent combustion force, and the loading frequency was 10 Hz and 25 Hz. In another study by Wang et al. [14], loads from 6.6 kN to 24.3 kN were used in the wear test, and the loading frequency and valve displacement were 10 Hz and 1.27 mm, respectively. However, these load levels were higher than those found in an engine and would

lead to possible misinterpretation. Consequently, the test conditions reflected the previous research and working conditions of a natural gas fuelled diesel, as well as the capabilities of the bench-top wear testing apparatus. The test temperatures of exhaust valve contact pairs and intake valve contact pairs were set at 700 °C and 400 °C, respectively. One type of seat insert was used in the test, and the test conditions are presented in Table 5. Other test parameters were set as follows: loading frequency was 10 Hz, valve lift was 5 mm, valve closing velocity was 150 mm/s. No misalignment and lubrication oil between the valve and seat insert were employed and the valve did not have any rotational motion during the test.
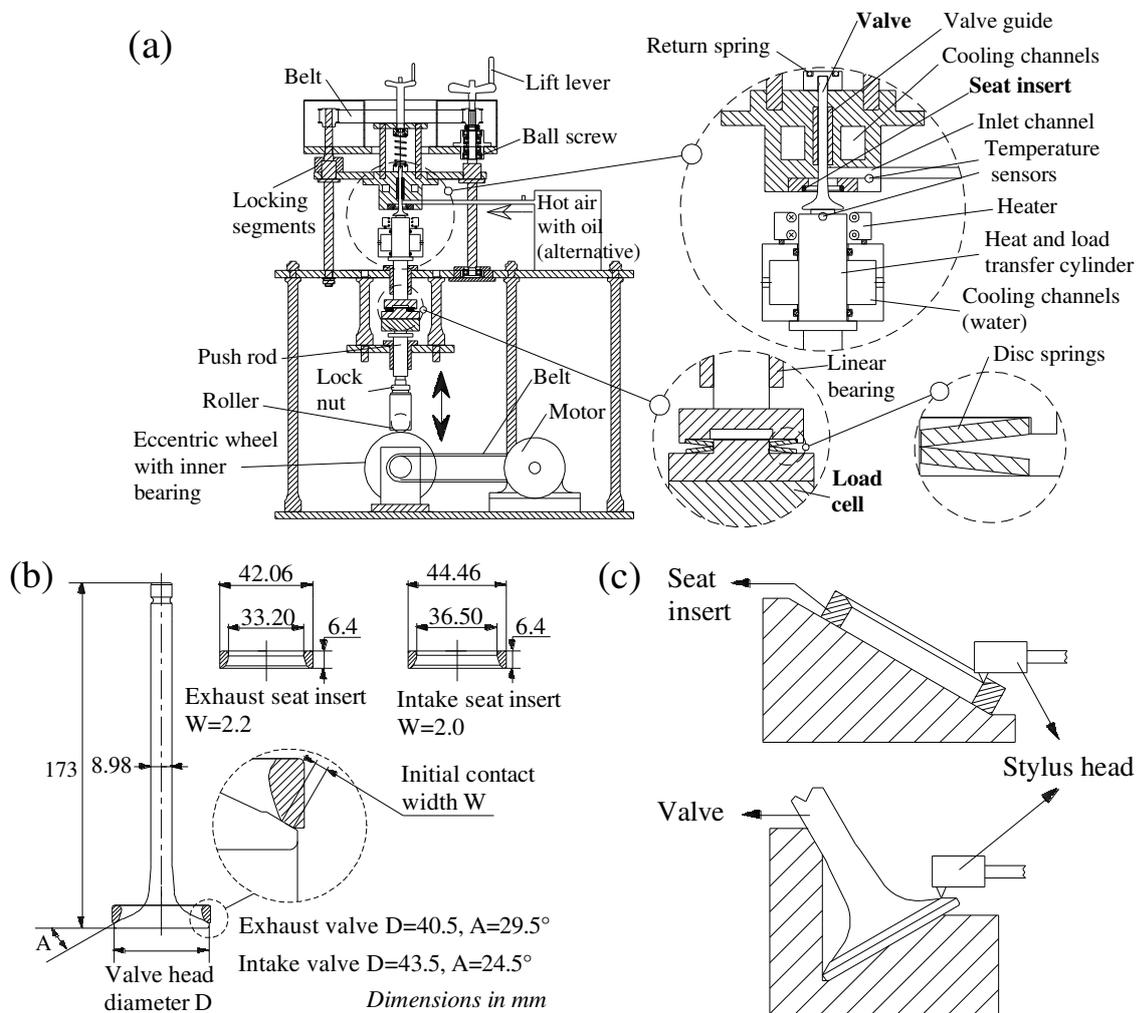

Fig. 2 (a) Schematic of the bench-top testing apparatus; (b) valve and seat insert geometry; (c) schematic of worn seating surface measurement through use of a profilometer.

Table 5 Conditions of wear test.

Specimen No.	Valve type	Valve name	Seat insert name	Temperature (°C)	Load (kN) 0–2 million cycles	2–3 million cycles
1	Exhaust valve	Valve 1	Seat Insert 1	700	5.1	6.2
2	Exhaust valve	Valve 2	Seat Insert 2	700	5.1	6.2
3	Intake valve	Valve 3	Seat Insert 3	400	5.1	6.2
4	Intake valve	Valve 4	Seat Insert 4	400	5.1	6.2

2.3 Stress analysis by FEM

As the combustion pressure in the cylinder applies a load on the valve head, micro-sliding occurs on the interface of valve seating face and seat insert. Based on the research results of Forsberg et al. [17] and Lewis and Dwyer-Joyce [2, 18], sliding in the sealing interface was one of the major reasons for the wear of engine valves and seat inserts. In addition, because the difference of valve material, test temperatures, initial contact width and angle of the seating face between the intake valves and exhaust valve, the relationship between sliding length and geometry of the valves and seat inserts had to be determined.

2.3.1 Simulation set-up 1

In the research work of Forsberg et al. [17], unique experimental data of sliding distance between engine valve and seat insert was acquired using a dedicated technique in a test-rig. The experimental data is complemented and validated by FEM simulations. To validate the sliding length simulation results in this work, the same geometry with one simulation setting of Forsberg et al. was modelled as follows: the valve head diameter was 41 mm, seating face angle was 30°, Young's modulus of valve material was 170 GPa, the coefficient of friction (COF) was

0.4, and the corresponding calculated combustion pressure was 20 MPa. The full contact length between valve and seat insert was set at 1.9 mm, 2.2 mm and 2.5 mm, respectively. The schematic diagram of simulation set-up 1 is presented in Fig. 3. The constraints are presented by the triangular symbols pointing the constrained direction of the relevant node. Note that the actual sliding length will be twice that of the simulated sliding length, because the surfaces will slide the same distance again during unloading [17].
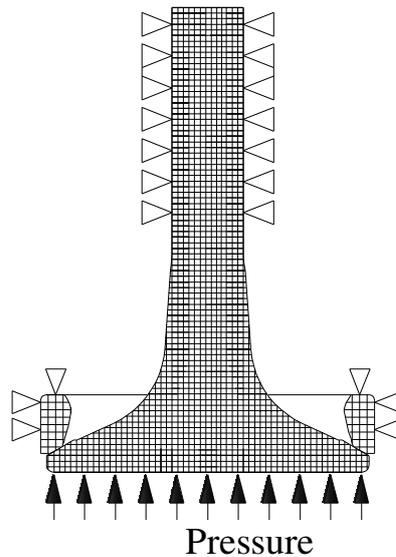

Pressure

Fig. 3 Schematic diagram of valve and inset insert FEM model for simulation set-up 1.

2.3.1 Simulation set-up 2

Based on the force conditions of the valve specimens during the bench-top test, the FEM model was established as illustrated in Fig. 4(a). No seating angle difference was set between the valve and seat insert. According to the geometry information of the valve and seat insert, a three dimensional model was established. Then, mechanical properties of the material at the tested temperature (Table 2) were used as inputs for the material properties of the FEM model. Element mesh refinement (with element size was set at 0.18 mm) was used in the contact zone to improve the calculation accuracy, as presented in Fig. 4(b). Between the seating zone of the

valve and seat insert contact elements with COF have been introduced.

In the former work of Qu et al. [19, 20], the friction and wear characteristics of 23-8N steel (austenitic engine valve steel) and 42Cr9Si2 steel (martensitic engine valve steel) against 3Cr3Mo3W2V die steel were respectively investigated at high temperature. At the temperature range from 400 °C to 650 °C, the average COF of 23-8N steel on steady state varied in the range from 0.35 to 0.65 [19]. At the temperature range from 200 °C to 400 °C, the average COF of 42Cr9Si2 steel on steady state varied in the range from 0.4 to 0.7 [20]. As reported by Sun et al. [21], the COF of TiAl alloy against GH3128 nickel-based superalloy was about 0.27 and 0.36 at 800 °C with two sliding speeds. The wear test of TiAl alloy against Si3N4 at elevated temperatures is reported by Kang et al. [22]. At the temperatures from 25 °C to 900 °C, the COF of TiAl slightly decreased from 0.42 to 0.39. Although the material of matched specimens in the sliding wear tests were not real seat insert materials, the value of COF could be used. Consequently, the COF of the contact element in simulation set-up 2 was respectively set in the range from 0.1 up to 0.7 with 0.1 intervals. The simulation was carried out using ANSYS 14.0 software.
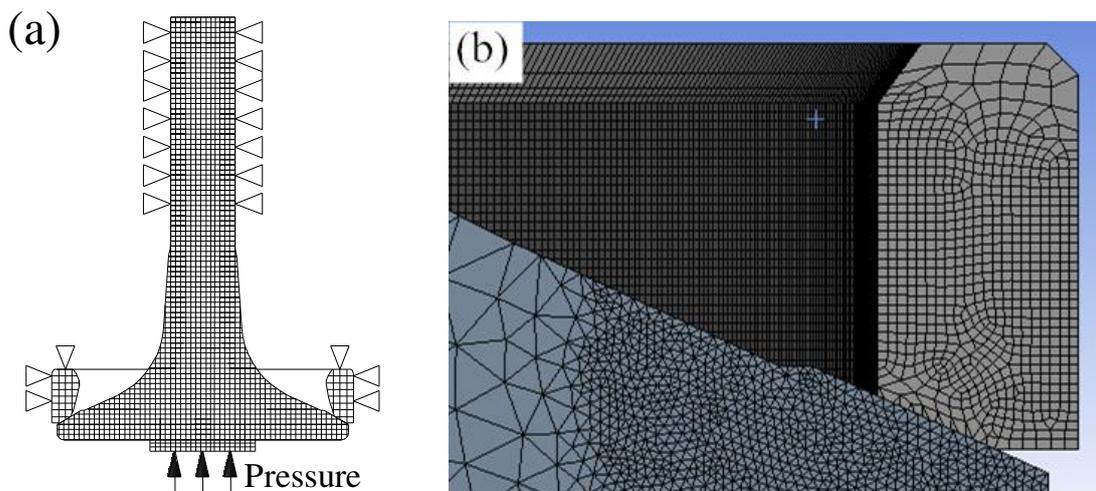

Fig. 4 (a) Schematic diagram of valve and inset insert FEM model for simulation set-up 2,(b)

schematic of element mesh refinement in the contact zone.

3. Results and discussion

3.1 FEM stress analysis results

3.1.1 Results of simulation set-up 1

The sliding distance of one of the simulation set-up 1 is presented in Fig. 5 (a), and the comparison of results between simulation set-up 1 and results from Forsberg et al. is presented in Fig. 5 (b). It could be inferred that, the FEM method employed in this paper could be verified by the results reported by Forsberg et al. [17].
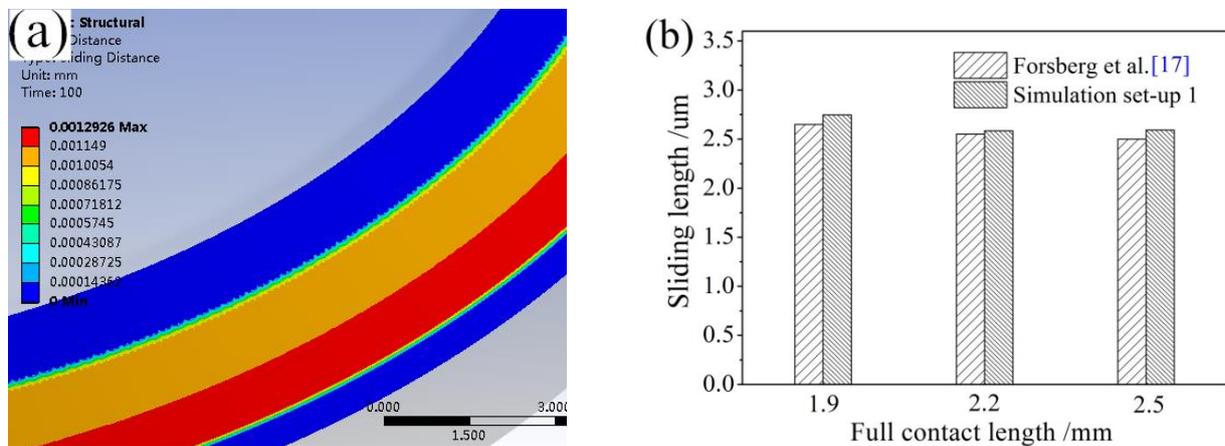

Fig. 5 (a) Sliding distance of simulation set-up 1; (b) the comparison of results of simulation set-up 1 and results from Forsberg et al. [17].

3.1.2 Results of simulation set-up 2

The typical FEM stress analysis result of von Mises stress distribution is presented in Fig. 6. Due to the loading on the valve head during the wear test, for the valve, except for the contact area, the concave area suffered the maximum stress, as indicated by the circle in Fig. 6. It is also reported by Worthen and Rauen that the concave area of engine valve withstood the maximum stress [23].
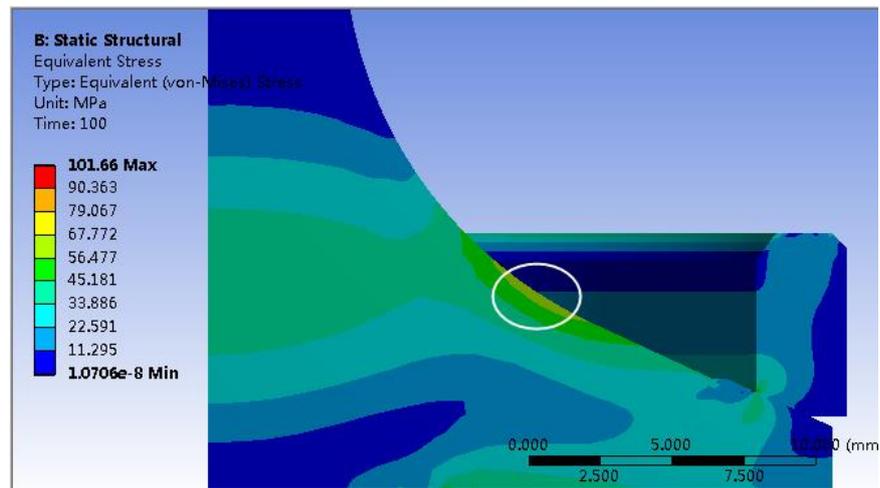
Fig. 6 Typical results of von Mises stress with a load of 6.2 kN.

The contact status of the surface of the interface between valve and seat insert is presented in Fig. 7 (a). Most of the contact area was in sticking status (red area), and the narrow area outside the red area was in sliding status, which is indicated by the arrow in the figure. The sliding distance is presented in Fig. 7 (b). The maximum sliding distance value occurred in the outside diameter direction, and a slightly lower value existed near the inside diameter direction. The sliding distance gradually decreased towards both the outside and inside contact area edges. The micro-sliding distance of four contact pairs with different COFs is presented in Fig. 8. With a same value of COF, the sliding length of exhaust valve contact pairs was higher than intake valves, due to the more serious performance degradation of materials at higher elevated temperatures. Although lack of real COF of the valve and seat insert material at elevated temperatures, the COF values of similar materials could be used. For instance, the COF of martensitic 42Cr9Si2 steel against 3Cr3Mo3W2V die steel at 400 °C was about 0.4 [20], so the COF of martensitic X85 steel at 400 °C was possible from 0.4 to 0.5. The very possible regions of COF values for four contact pairs are indicated in Fig. 8. Then, the corresponding calculated sliding lengths were obtained. It is found that the sliding length of Valve 1 was almost same as

that of Valve 2, and the sliding length of Valve 4 was higher than that of Valve 3. As the total number of impact cycles increased, the full contact length between valve and seat insert increased, the sliding distance slightly decreased under the same loads.
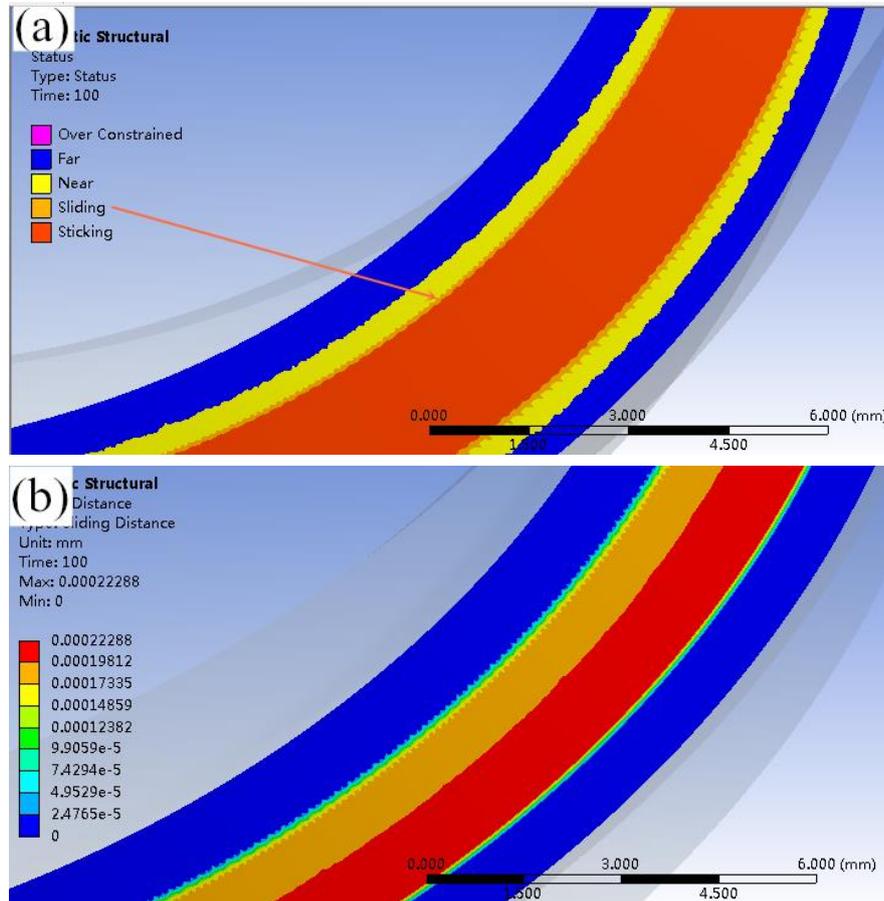

Fig. 7 Typical results of simulation set-up 2: (a) contact status; (b) contact sliding distance.
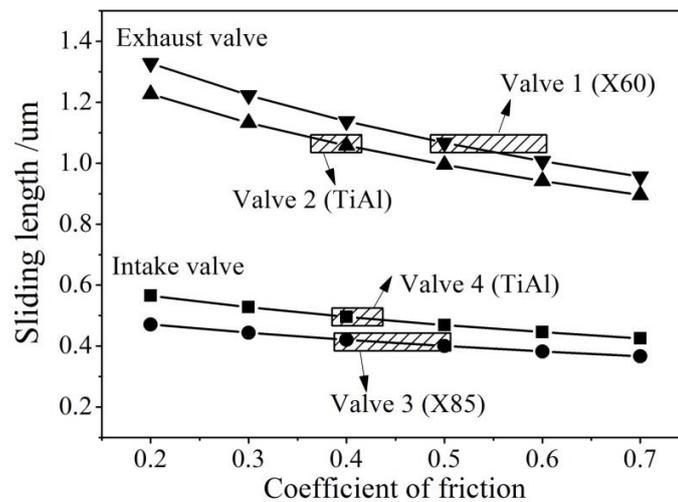

Fig. 8 The sliding distance of four contact pairs under the different coefficient of friction.

The wear volume result from sliding could be calculated by Archard's wear equation, as presented in Equation (1) [24].

$$W = \frac{KLS}{H} \tag{1}$$

where W is total wear volume, K is wear coefficient, L is total normal load, S is sliding length, and H is the hardness of the softest surface. During the bench-top wear test, the loads of the four valve contact pairs were kept the same. Thus, the wear loss generated by sliding was influenced by the sliding length and the hardness of the softest materials. Based on Archard's wear equation and the results of sliding length in Fig. 8 and the hot hardness of the engine valve and seat insert in Table 3, it is inferred that: the wear loss of exhaust contact pairs would be higher than that of the intake contact pairs, the wear loss of the TiAl exhaust valve would be lower than that of the X60 exhaust valve.

3.2 Wear resistance behaviour

3.2.1 Wear scar of valve seating face

The main problem is the wear loss of the seating face of the valve and seat insert. Wear loss is a complex process which is affected by materials and test conditions and the time (impact cycles). An image of the surface of the Valve 2 seating face after two million impact cycles is presented in Fig. 9(a). The wear scar profile of Valve 2 after three million impact cycles is shown in Fig. 9(b). Based on the 2D wear scar profile, the wear scar area was calculated. Fig. 9(c) reveals the wear scar area of the four valve seating faces after three million impact cycles, and error bar in the figure represents the standard deviation of the wear scar area. For exhaust valves, compared to the heat resistant steel valve (X60), the wear scar area of the TiAl valve decreased from 0.2701 mm^2 to 0.2032 mm^2. since the hardness of TiAl alloy was higher than X60 steel at

700 °C. For intake valves, compared to heat resistant steel valve (X85), the wear scar area of TiAl valve increased from 0.0875 mm^2 to 0.3588 mm^2. The low wear loss of Valve 3 can be attributed to the quenching treatment on valve seating face, the material could obtain high hardness at 400 °C, leading to a better wear resistance. For the two TiAl valves, however, the wear loss of valve at 700 °C was lower than that at 400 °C, and cannot be explained by the hardness of materials, so will be discussed later in conjuction with the wear mechanisms.
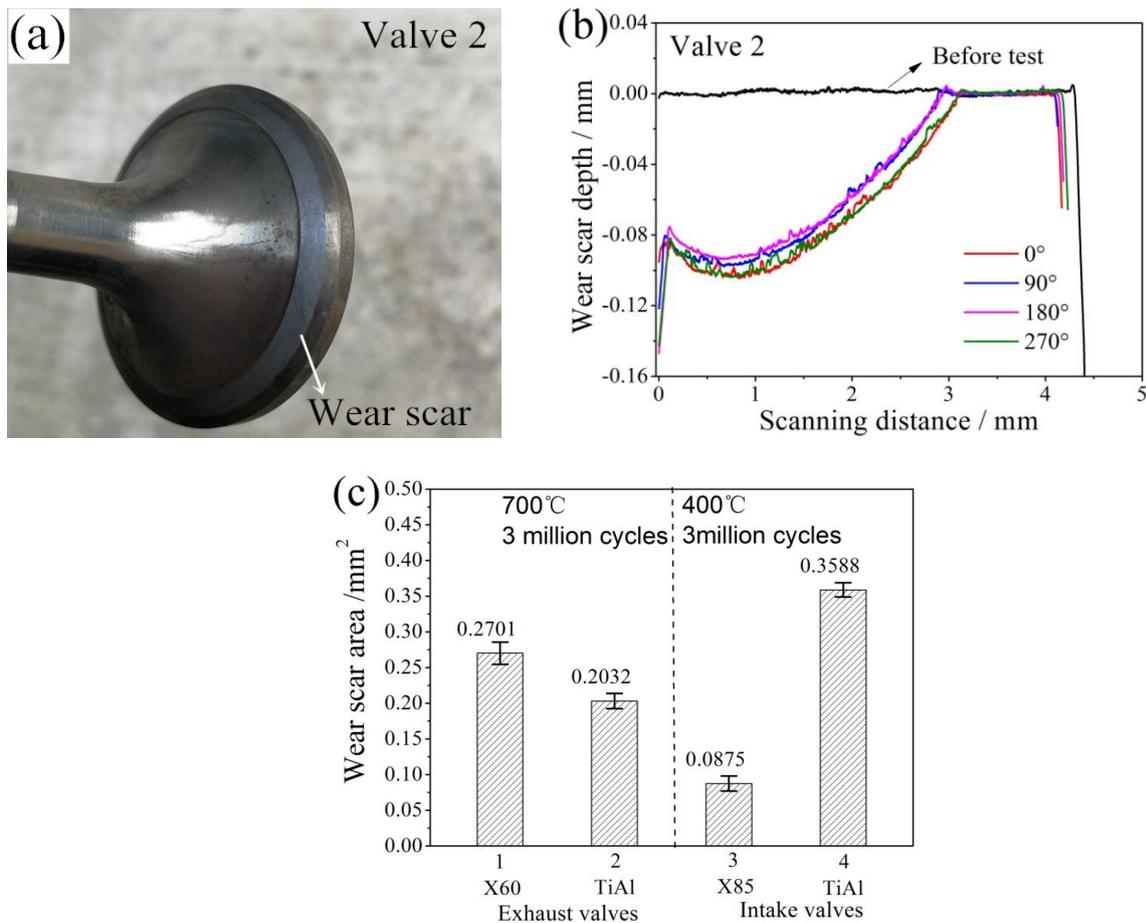

Fig. 9 (a) Valve 2 after two million impact cycles; (b) the wear scar profile of Valve 2 after three million impact cycles; (c) wear scar area of the four valve seating faces.

3.2.2 Wear scar of seat insert

Fig.10 (a) presents the wear scar profiles of a seat insert seating faces after a wear test. The average value of wear scar area of the four seat insert seating faces is presented in Fig.10 (b), the

error bars represent the standard deviation of the calculated wear scar area. It was found that the material loss magnitude of seat insert was different with the matched valve. The wear loss of exhaust seat inserts was generally higher than intake seat inserts, due to the higher test temperature. Compared to the wear loss of Seat Insert 1 and Seat Insert 3, the wear loss of Seat Insert 2 and Seat Insert 4 (matched with TiAl valves) obtained a higher variation range at different measurement points, indicating that more serious misaligned wear scars occurred.
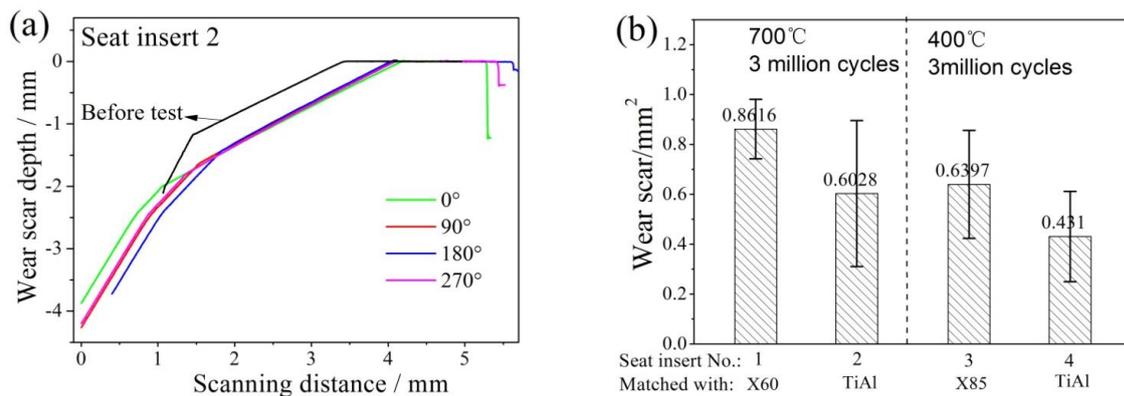

Fig.10 (a) The wear scar profile of Seat Insert 2; (b) wear scar area of the four seat insert seating faces.

3.2.3 Total wear of the contact pair

Fig. 11 presents the total wear area of four contact pairs. The wear loss of exhaust contact pairs was higher that intake contact pairs, which was same with the analysis results of simulation 2. For every contact pair of valve and seat insert, the wear scar area of a seat insert occupied a higher proportion than a valve. For exhaust valve contact pairs, the total wear of the TiAl valve contact pair was significantly lower than the austenitic steel valve contact pair (X60). However, for the intake valve contact pairs, the total wear of the TiAl valve contact pair was even a little higher than martensitic steel valve contact pair (X85).
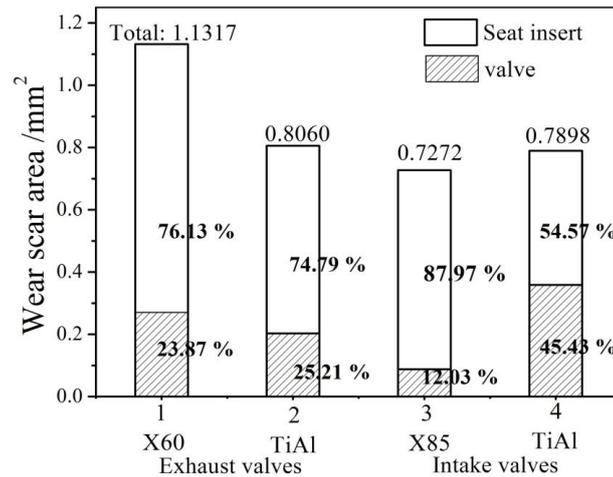
Fig. 11 Total wear area of four contact pairs of valve and seat insert.

Valve recession was calculated as per the method put forward by Lewis and Dwyer-Joyce [18], and the schematic of valve recession calculation is presented in Fig. 12(a). The valve recession followed the variation trend of total wear of contact pairs, as shown in Fig12(b). After an adjustment of valve stem clearance, the permissible maximum value of valve recession for the natural gas fuelled diesel is 1.3 mm. Due to the dry sliding and impact test conditions in the bench-top wear tests, the rate of valve recession was significantly higher than that in an actual engine. The lower rate of valve recession in a real operation engine is attributed to the protective tribofilms formed on the contact surfaces between valves and seat inserts [25].

As reported by Ouyang et al. [9], after a 48 hour test on a diesel engine, compared to heat resistant steel engine valve (21-4N), the valve recession of TiAl exhaust engine valve decreased to one-eighth. In addition, it is also reported by Li and Luo [10], the valve recession of TiAl valves was almost same with the original exhaust valve recession in a same diesel. Compared to the work conditions of valves in the dynamometer engine test, although it is hard to achieve the same test conditions in the bench-top test in this work, the results still could be used as a quick and indicative tool to evaluate the tribological performance of new materials for engine valves.

Consequently, it is concluded that the TiAl alloy is probably a potential solution for exhaust valves of a natural gas fuelled diesel. However, TiAl alloy is probably not suitable for intake valves.
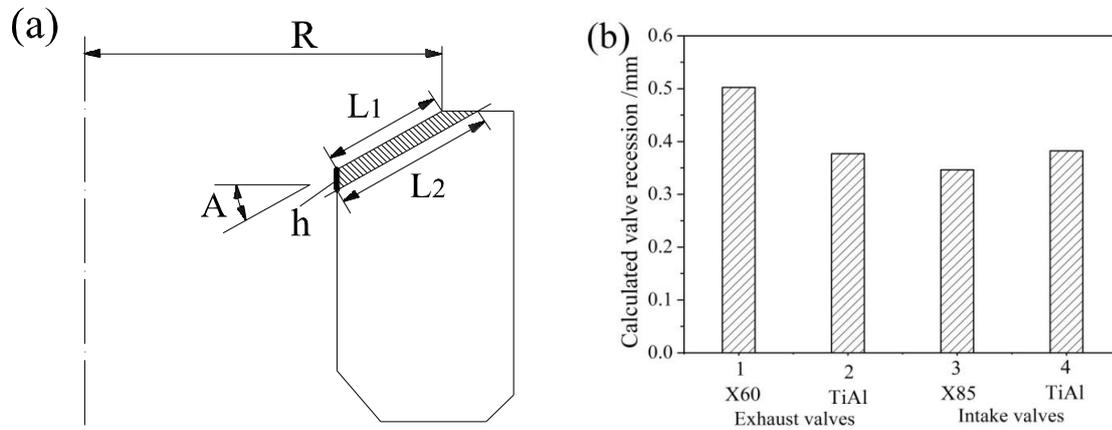

Fig. 12 (a) Schematic of valve recession calculation; (b) valve recession of specimens.

3.3 Worn surface and wear mechanisms

3.3.1 Worn surface of valve seating face

Fig. 13 and 14 exhibit the wear morphology found on the seating face of Valve 1 and Valve 3, respectively. The corresponding EDS results of worn surfaces and non-contact surfaces are listed in Table 6. Adhesive traces were found on the worn surfaces of Valve 1, as presented in Fig. 13(b). Due to the softening of the heat resistant steel (X60) and the descending of its strength at 700 °C, the debris generated from the closing impact began to be oxidized, forming poorly adherent oxide layers at the high temperature test conditions. Oxide layers were broken by shearing stress under the sliding action of the rubbing surfaces. EDS results (Table 6) of the adhesive traces show that they contained high oxygen content. Meanwhile, compared to the non-contact area of the valve seating face, copper and tungsten e were also detected on the worn surface (Table 6), indicating that the seat insert material was transferred to the valve seating face and that the adhesion was an oxygen–rich compound. It is also reported by Mascarenhas et al.

[26], seat insert materials were detached and adhered on the valve's surfaces.

Compared to the Valve 1, the tribological layers on the worn surface of Valve 3 was shown to be more compact, as presented in Fig. 14(b) and (c). Thanks to the quenching treatment for Valve 3 seating face, the material could obtain high hardness at 400 °C, leading to a better wear resistance of the seating surface and its oxide layers. Thus, the wear loss of Valve 3 held the minimum value, but the matched Seat Insert 3 suffered the maximum wear loss (wear loss proportion of corresponding contact pair).
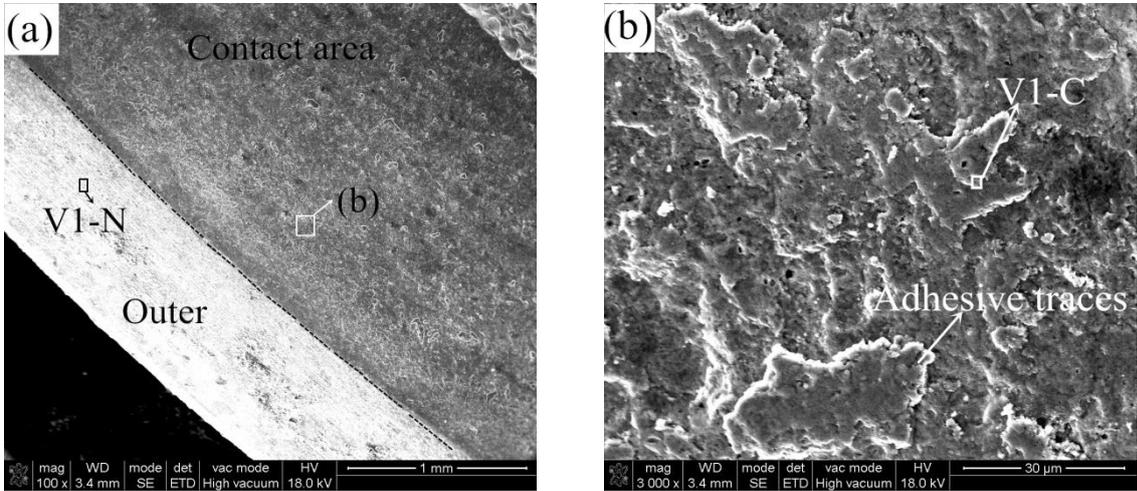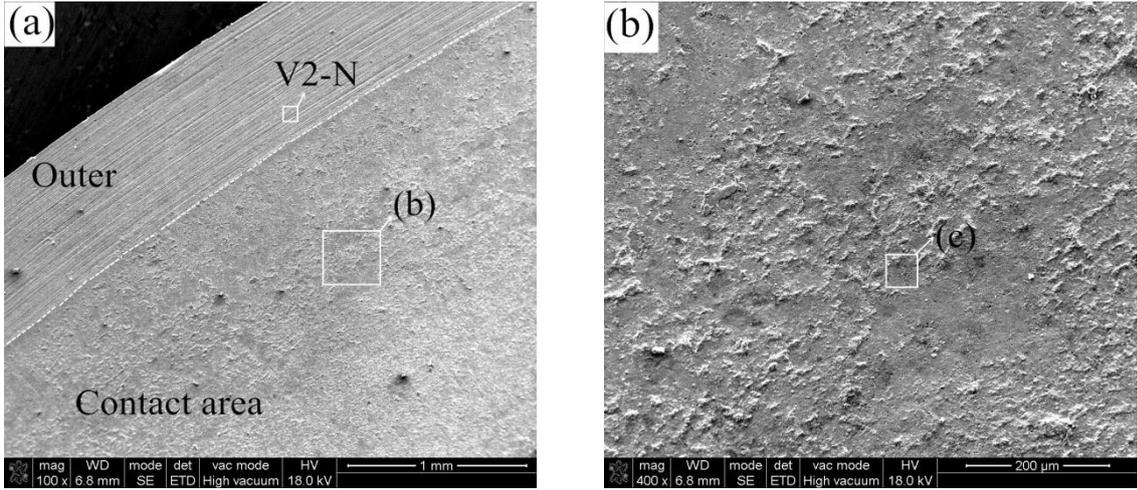

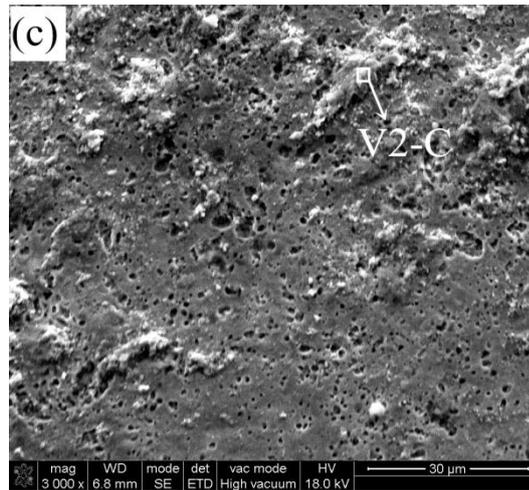Fig. 13 Worn surfaces of Valve 1 seating face and EDS test area.

Fig. 14 Worn surfaces of Valve 3 seating face and EDS test area.

Table 6 EDS results of the areas on valve seating face (wt. %).

Specimen	Area	C	O	Si	V	Cr	Mn	Fe	Ni	Mo	Cu	W
Valve 1	V1-N	9.79	5.90	0.31	0.25	14.04	0.60	66.63	0.45	2.03	–	–
Valve 1	V1-C	8.12	22.96	–	0.75	12.21	–	46.14	–	4.55	3.81	1.6
Valve 3	V3-N	12.70	20.98	–	1.08	23.7	6.28	35.48	–	–	–	–
Valve 3	V3-C	6.79	32.10	–	0.67	8.35	3.15	38.59	0.81	5.44	2.11	2.00

3.3.2 Worn surface of seat insert

Impact and micro sliding are the main reasons to describe the wear loss of engine valve contact pairs [2, 17, 18]. With the increase of impact cycles, the wear debris may be generated from both sides of the sealing interface. Then, these were compacted into thin layers that were attached to the surfaces by contact adhesion. The worn surfaces of the four seat insert are presented in Fig. 15–18, and the corresponding EDS results of worn surfaces and non-contact surfaces are listed in Table 7. Adhesive wear is characterized by bonding and subsequent breakage occurring alternately between sliding materials. Adhesive traces were identified on the worn surfaces of exhaust seat inserts, as presented in Fig. 15(b) and Fig. 16(b). EDS results (Table 7) of the

adhesive traces show that they contained high oxygen content, so the wear rate was accelerated by some type of oxidative wear due to the elevated temperatures. Combined with the analysis of the worn surface of Valve 1, the wear mechanisms of exhaust valve contact pairs are concluded to be oxidative wear combined with adhesive wear.

The hardness of the TiAl alloy kept almost the same when the temperature lower than 700 °C (Table 3), thus the hardness of Valve 2 and Valve 4 were at a same level. However, the hardness of Seat Insert 2 was inferred to be much lower than Seat Insert 4. Compared to Valve 4, the lower wear loss of Valve 2 may be attributed by the lubrication role of oxide layers on its worn surface. The oxide layer acted as a "crash pad" to avoid the direct contacting (metal to metal) of contact pairs to some extent. Because the lower hardness of Seat Insert 2, its wear loss was higher than Seat Insert 4. At last, the total wear of the TiAl exhaust valve contact pair was a bit higher than the TiAl intake valve contact pair. Surface treatment should be introduced to the TiAl valve, for instance, plasma carburizing is effective in improving wear resistance on the valve stem and seating face [5].

Material transfer phenomena were also identified on the worn faces of seat inserts. As presented in Table 7 (area of S2-C and S4-C), the Aluminium and Titanium element were also detected on the Seat Insert 2 and Seat Insert 4, since they were matched with TiAl valves. Based on the EDS results from Table 6 and 7, it is proved that the transferring behaviour of materials between the valve seating surface and seat insert indeed existed. The associated wear mechanism thus included adhesive wear.

Both peeling and adhesive traces of materials were found on the worn surfaces of Seat Insert 3, as presented in Fig. 17(b). The adhesions of debris on the worn surface of Seat Insert 4 were

shown to be more compact, as presented in Fig. 18(b). The worn surfaces of Seat Insert 3 and 4 also contained oxygen content to some extent, as presented in Table 7. Compared to the exhaust valve contact pairs tested at 700 °C, the contact adhesion on the seating face of intake valve and seat insert, as well as the generated wear debris could obtain a higher hardness at 400 °C. The contact adhesion would be broken, and more likely due to the increased weakening of the surface through oxidative wear, and fragments of material detach from the worn surfaces and act as third bodies. Consequently, it is observed the micro-plowing and ground fragments on the worn surface of Seat Insert 3, as presented in Fig. 17(c) and (d). The predominant wear mechanisms can be identified as abrasive wear and adhesive wear.
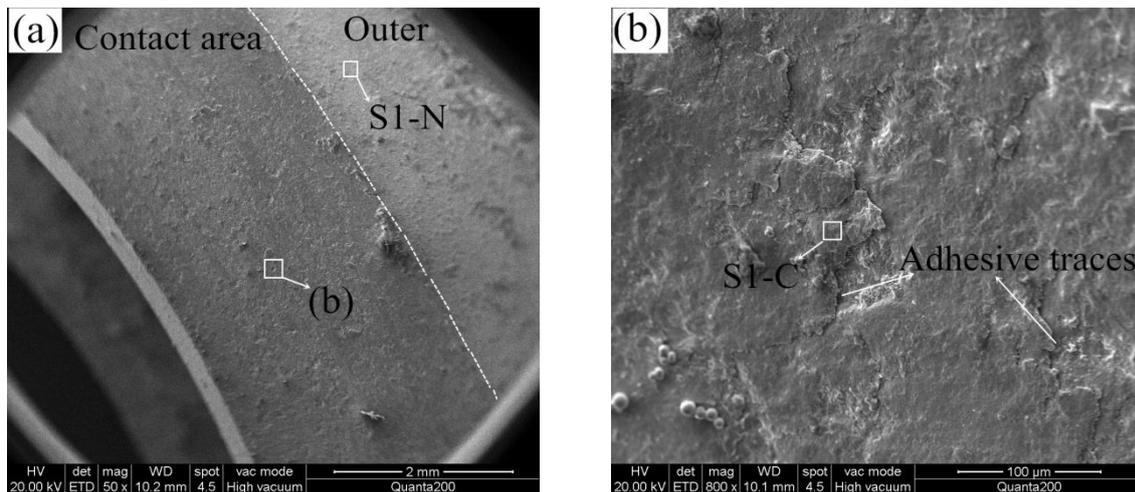

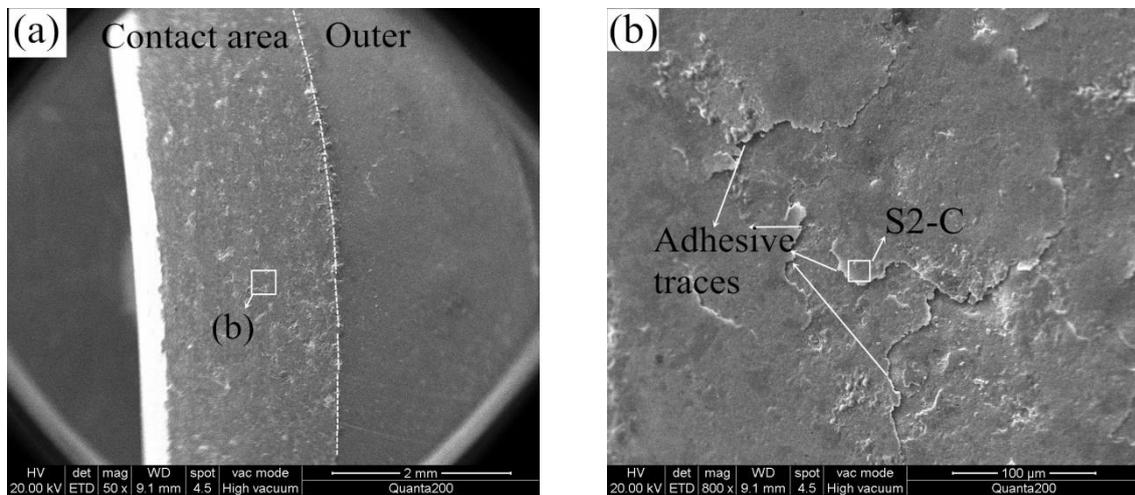Fig. 15 Worn surfaces of Seat Insert 1.

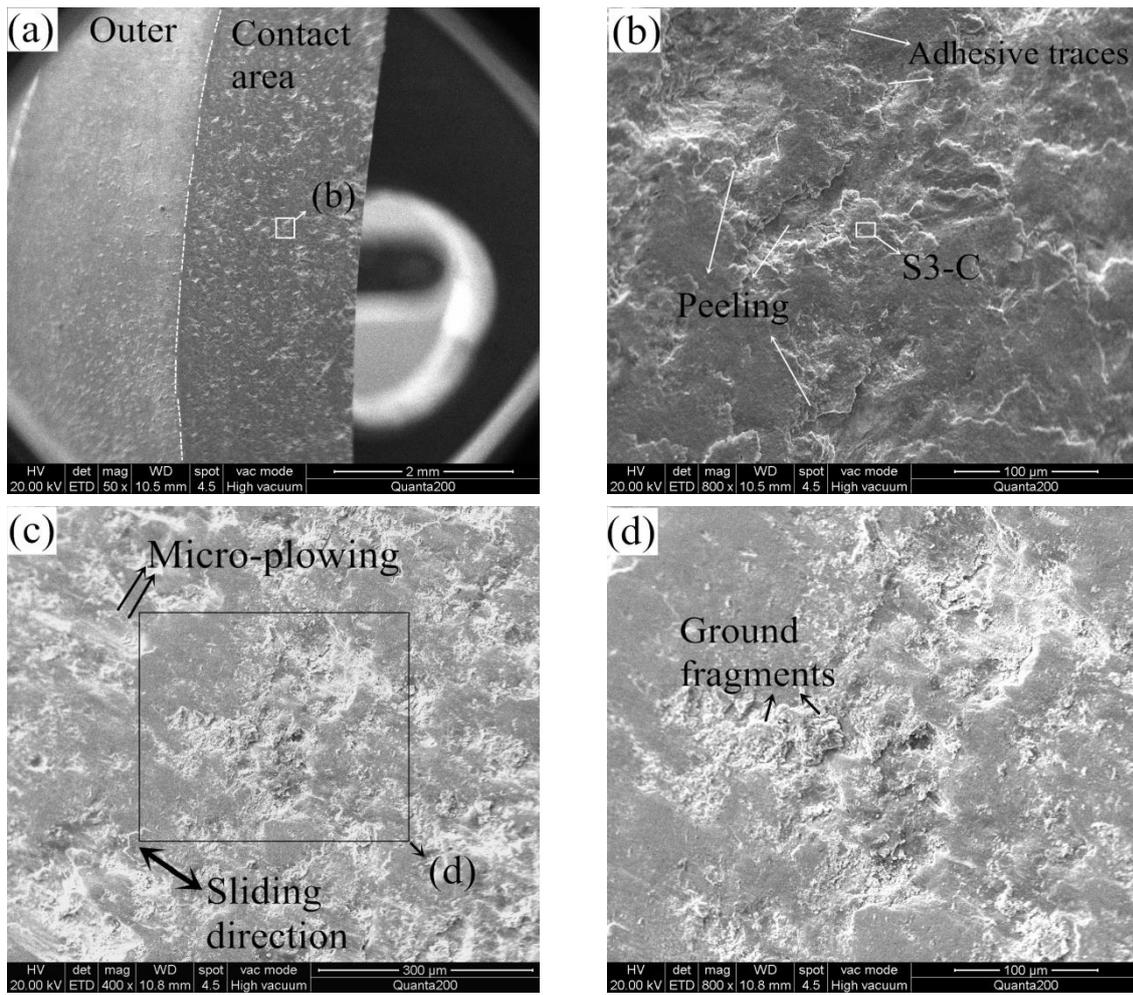Fig. 16 Worn surfaces of Seat Insert 2.
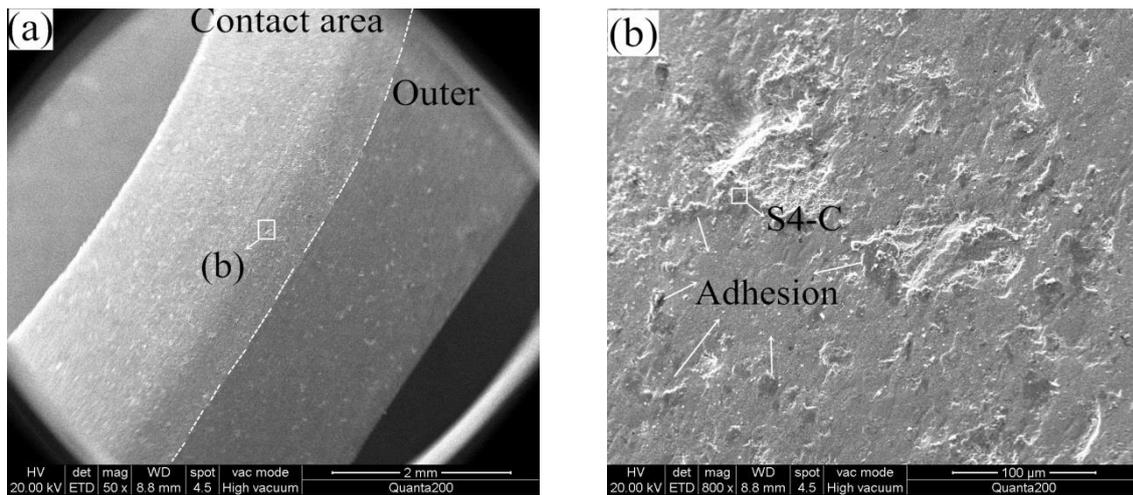

Fig. 17 Worn surfaces of Seat Insert 3.

Fig. 18 Worn surfaces of Seat Insert 4.

Table 7 EDS results of the areas on seat insert seating face (wt. %).

Specimen	Area	O	V	Cr	Mn	Fe	Co	Ni	Mo	Cu	W	Al	Ti
Seat Insert 1	S1-N	3.58	3.23	6.16	–	62.08	8.12	1.48	4.94	6.62	3.80	–	–
Seat Insert 1	S1-C	37.32	2.04	4.77	0.66	43.25	5.38	1.03	–	4.77	0.77	–	–
Seat Insert 2	S2-C	21.43	1.31	4.01	2.10	28.64	3.86	–	5.72	11.26	2.59	4.12	14.95
Seat Insert 3	S3-C	20.14	1.12	6.50	–	53.16	6.55	–	3.13	5.95	3.45	–	–
Seat Insert 4	S4-C	6.62	–	2.19	5.02	20.01	1.98	–	2.65	3.69	1.02	17.89	38.93

4. Conclusions

The wear behaviour of heat resistant steel engine valves and TiAl engine valves were compared through bench-top wear tests. The conclusions can be drawn as follows:

(1) Compared to the austenitic exhaust valves tested at 700 °C, the TiAl valve had better wear resistance, the wear loss decreased by 24.8 %. The predominant wear mechanism is considered a combination of oxidative wear and adhesive wear.

(2) Compared to the martensitic intake valves tested at 400 °C, the wear loss of the TiAl valve was four times as much as martensitic intake valves. The predominant wear mechanism can be identified as abrasive wear and adhesive wear

(3) The TiAl exhaust valve is a potential solution for a natural gas fuelled diesel ICE.

Acknowledgements

Conflicts of Interest: The authors declare no conflict of interest.

References

[1] YS Wang. Introduction to engine valvetrains. Warrendale: SAE International; 2007.

[2] R Lewis, RS Dwyer-Joyce. Automotive engine valve recession. London: Engineering research series, 2002.

[3] M Badami, F Marino. Fatigue tests of un-HIP'ed γ-TiAl engine valves for motorcycles. Int J Fatigue 2006; 28:722–732.

[4] H Clemens, S Mayer. Intermetallic titanium aluminides in aerospace applications– processing, microstructure and properties. Mater High Temp 2016; 33(4-5): 560–570.

[5] K Maki, A Ehira, M Sayashi, T Sasaki, T Noda, M Okabe, S Isobe. Development of a high-performance TiAl exhaust valve. SAE 960303, 1996.

[6] WE Dowling, Jr JE Allison, LR Swank, AM Sherman. TiAl-based alloys for exhaust valve applications. SAE 930620, 1993.

[7] M Blum, G Jarczyk, H Scholz, S Pleier, P Busse, HJ Laudenberg, K Segtrop, R Simon. Prototype plant for the economical mass production of TiAl-valves. Mat Sci Eng A-Struct 2002; 329–331: 616–620.

[8] PX Fu, XH Kang, YC Ma, K Liu, DZ Li, YY Li. Centrifugal casting of TiAl exhaust valves. Intermetallics 2008; 16: 130–138.

[9] HW Ouyang, BY Huang, YH He, Y Liu, AX Li. Development of TiAl-based automotive engine exhaust valves. The Chinese Journal of Nonferrous Metals 2000; 10 (Suppl 1): 60–63 [in Chinese].

[10] JM Li, ZR Liu. The study of exhaust valve of Tilanium-aluminium alloy in diesel engine testing. Journal of Hunan university (Natural Sciences Edition) 2001; 28(2): 32–34 [in Chinese].

[11] ZR Zhang, YS Sun, XJ Lin, DQ Mo, G Sun, G Chen, DT Su, ZY Li, WQ Qiu, BY Wang, JP Liu. A forming technology for hollow head & sodium filled engine valve which based on cross wedge rolling to produce workblank. China patent, ZL 201510236950.9. 2017-10-27 [in Chinese].

[12] FQ Lai, SG Qu, Y Duan, R Lewis, T Slatter, LM Yin, XQ Li, HH Luo, G Sun. The wear and fatigue behaviours of hollow head & sodium filled engine valve. Tri. Int. 2018; 128:75–88.

[13] FQ Lai, SG Qu, LM Yin, GH Wang, ZX Yang, XQ Li. Design and operation of a new multifunctional wear apparatus for engine valve train components. Proc. IMechE, Part J: J Engineering Triblogy 2018; 232(3): 259–276.

[14] MS Baniasad, E Khalil, F Shen. Exhaust valve thermal management and robust design using combustion and 3d conjugate heat transfer simulation with 6-sigma methodology. SAE 2006-01-0889, 2006.

[15] KJ Chun, JH Kim, JS Hong. A study of exhaust valve and seat insert wear depending on cycle

numbers. Wear 2007; 263: 1147–1157.

[16] YS Wang, S Narasimhan, JM Larson, JE Larson. GC Barber. The effect of operating conditions on heavy duty engine valve seat wear. Wear 1996; 201:15–25.

[17] P. Forsberg, D. Debord b, S. Jacobson. Quantification of combustion valve sealing interface sliding – A novel experimental technique and simulations. Tri. Int. 2014; 69:150–155.

[18] R Lewis, RS Dwyer-Joyce. Wear of diesel engine inlet valves and seat inserts. Proc. IMechE, Part D: J of Automobile Engineering 2002; 216(3): 205–216.

[19] SG Qu, LM Yin, FQ Lai, et al. High temperature friction and wear properties of 23-8N valve steel. Journal of South China University of Technology (Natural Science Edition) 2017; 45(12):.78–84 [in Chinese].

[20] SG Qu, LM Yin, FQ Lai, CW Xiao, XQ Li. Study on High temperature friction and wear characteristics of 4Cr9Si2 valve steel. Advances in Mechanical Design. ICMD 2017. Mechanisms and Machine Science, Springer, Singapore, 2017; 55: 1535-1546.

[21] DL Sun, T Sun, Q Wang, XL Qin, LL Guo. Friction and wear properties of TiAl and Ti2AlN/TiAl composites at high temperature. J. Wuhan Univ. Technol. 2013; 28(5): 1023–1028.

[22] K Yang, XL Shi, YC Huang, ZH Wang, YF Wang, A Zhang, QX Zhang. The research on the sliding friction and wear behaviours of TiAl-10 wt% Ag at elevated temperatures. Mater. Chem. Phys. 2017; 186: 317–326.

[23] RP Worthen, DG Rauen. Measurement of valve temperatures and strain in a firing engine. SAE 860356, 1986.

[24] JF Archard. Contact and rubbing of flat surfaces. J Appl Phys 1953; 24:981–988.

[25] JM Li, ZR Liu. The study of exhaust valve of Tilanium-aluminium alloy in diesel engine testing. Journal of Hunan university (Natural Sciences Edition) 2001; 28(2): 32–34 [in Chinese].

[26] LAB Mascarenhas, JDO Gomes, VE Beal, AT Portela, CV Ferreira, CA Barbosa. Design and operation of a high temperature wear test apparatus for automotive valve materials. Wear 2015; 342–343: 129–137.